JOURNAL OF MATERIALS SCIENCE 29 (1994) 949–953

Electrolytic depositions of calcium phosphates on substrate

H. MONMA
National Institute for Research in Inorganic Materials, Tsukuba-shi, Ibaraki, 305 Japan

Calcium phosphate deposition layers on cathode substrates were prepared by electrolysing acidic $Ca(H_2PO_4)_2 \cdot H_2O$ (MCP) solutions of 0.02–0.21 mol dm^{-3} added with and without $NaNO_3$ at cathode currents of 2–200 mA cm^{-2} at 20–90 °C. At relatively high MCP concentrations and low currents, $CaHPO_4 \cdot 2H_2O$ and $CaHPO_4$ plate-like crystals were deposited below and above ~30 °C, respectively. With increasing current, the deposits became fine. On further increasing the current and/or decreasing the MCP concentration, apatite deposition occurred. The addition of $NaNO_3$ facilitated the formation of apatite. Deposited apatites were very fine grains and had a calcium-deficiency of ~1.50 in the Ca/P molar ratio.

1. Introduction

Because of the biocompatibility of hydroxyapatite (HAp), coatings of HAp and related calcium phosphates on biomechanically compatible metals and ceramics have been of great interest. The composition of HAp is expressed by stoichiometric $Ca_{10}(PO_4)_6(OH)_2$ and nonstoichiometric $Ca_{10-x}(HPO_4)_x(PO_4)_{6-x}(OH)_{2-x} \cdot nH_2O; 0 < x \leqslant 1$. Many methods such as plasma-spraying, sputtering, electrophoresis, spark discharge in electrolyte, spontaneous deposition in solution, dipping and spray-pyrolysis, have been employed for the preparation of HAp coatings or thin films. Recently, electrolytic techniques for calcium phosphate coatings have been introduced by Redepenning and McIsaac [1] and Shirkhanzadeh [2]. In the former report, brushite ($CaHPO_4 \cdot 2H_2O$) coatings on cathodes were prepared by electrolysing galvanostatically a calcium phosphate solution (pH 3.50), and in the latter HAp coatings, by electrolysing potentiostatically a calcium phosphate solution (pH 4.4) with added NaCl. Because of the decreasing solubility of calcium phosphates with increasing pH, calcium phosphates are thought to be deposited on the cathode as a result of pH increases in the vicinity of cathode, by the reduction of H^+ ions accompanying the generation of H_2 gas and OH^- ions.

In the present work, with a view to clarifying further details on the electrolytic formation of calcium phosphates, products deposited on cathode substrates under various electrolytic conditions were investigated with respect to products and their formation region, morphology, compositional and thermal characteristics.

2. Experimental procedure

Electrolysis runs were carried out at constant cathode currents of 2–200 mA cm^{-2} at temperatures of 20–90 °C for appropriate times within 60 min. The electrolytes used were acidic 0.02–0.21 mol dm^{-3} $Ca(H_2PO_4)_2 \cdot H_2O$ (MCP) solutions (50 ml) added with and without $NaNO_3$ (7.0 g). The electrodes were a platinum plate of dimensions 0.1 mm × 35 mm as an anode and a SUS304 stainless steel (in certain runs SUS316L or titanium) plate of dimensions 0.1 mm × 8–15 mm as a cathode. The resulting deposits on the cathode were examined as deposited, after drying in air or as powders scraped from the cathode with a Philips PW1700 X-ray diffractometer (XRD), a Digilab FTS-60 infrared spectroscope equipped with a reflection–absorption accessory for thin films (RAS-IR) and a KBr-disc accessory for scraped powders (KBr-IR), an Akashi ISI-DS130 scanning electron microscope (SEM) equipped with a Philips PV9900-ECON3 energy dispersive X-ray spectrometer (EDX) and a Shinku-Riko TGD-7000 thermogravimetric analyser (TG). Table I lists the deposited samples and their preparative conditions.

3. Results and discussion

3.1. Formation regions of the products

First, the deposition products at various temperatures were examined at a constant MCP concentration of 0.21 mol dm^{-3} at an electrolysis current of 6 mA cm^{-2} (Fig. 1). Brushite ($CaHPO_4 \cdot 2H_2O$) was deposited at temperatures below 25–35 °C and monetite ($CaHPO_4$) at higher temperatures. No apatite formation was observed up to 90 °C. Both products generally precipitated at lower pH values than that for apatite. Therefore, the pH increase in the vicinity of the cathode was supposed to be insufficient to form apatite under the electrolysis conditions, even though $NaNO_3$ was added.

Next, for the purpose of obtaining information on apatite deposition, the electrolysis current and MCP concentration were varied. The formation regions of calcium phosphates obtained at 45 °C are shown in

0022–2461

TABLE I Preparation of calcium phosphate deposits

Sample	Deposition product	Electrolyte		Electrolysis		
		MCP (mol dm^{-3})	Additive	Cathode current (mA cm^{-2})	Temperature (°C)	Time (min)
B1	$CaHPO_4 \cdot 2H_2O$	0.21	–	6	45	12
B2	$CaHPO_4 \cdot 2H_2O$	0.21	–	80	45	2
M1	$CaHPO_4$	0.21	–	6	87	5
M2	$CaHPO_4$	0.21	$NaNO_3$	15	50	3
Ap1	Apatite	0.02	–	25	25	60
Ap2	Apatite	0.04	–	20	45	10
Ap3	Apatite	0.21	$NaNO_3$	145	45	5
Ap4	Apatite	0.21	$NaNO_3$	200	45	5
ACP1	ACP	0.02	–	80	45	5

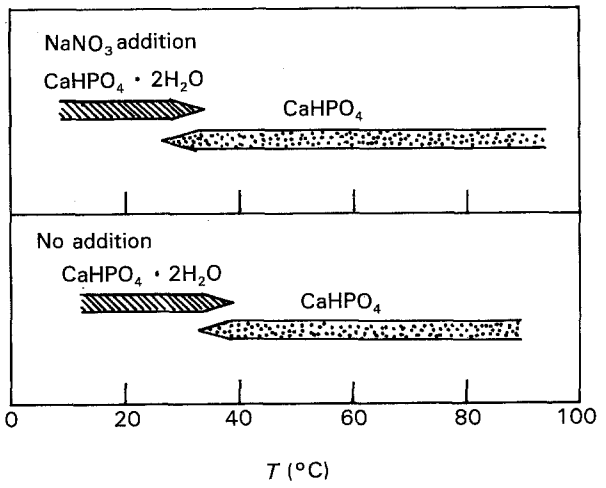

Figure 1 Changes in deposition phase with electrolysis temperature (0.21 mol dm^{-3} MCP, 6 ± 1 mA cm^{-2}).

Fig. 2. Apatite and amorphous calcium phosphate (ACP) depositions were achieved at dilute concentrations or high electrolysis currents. The composition of ACP is generally expressed as $Ca_3(PO_4)_2 \cdot nH_2O$ [3, 4]. Examples of IR spectra and XRD patterns for as-deposited layers are shown in Figs 3 and 4, respectively. IR bands at 1100–1000 (ν_3), 960 (ν_1), 600 (ν_4), 570 (ν_4) and 470 cm^{-1} (ν_2) are assigned to PO_4 vibrations in apatite. The band around 870 cm^{-1} is characteristic of the HPO_4 substituting the PO_4, and both the 870 and 1400–1500 cm^{-1} bands are typical of B-type CO_3^{2-} -containing apatite [5]. ACP has a single band at 570 cm^{-1} [4], not a split band as in apatite. Most apatite deposits had no or very weak bands due to OH (stretching, 3570 cm^{-1}, libration 630 cm^{-1}). Because H_2O molecules are able to replace the OH groups [6], the OH sites might be mostly occupied by H_2O molecules.

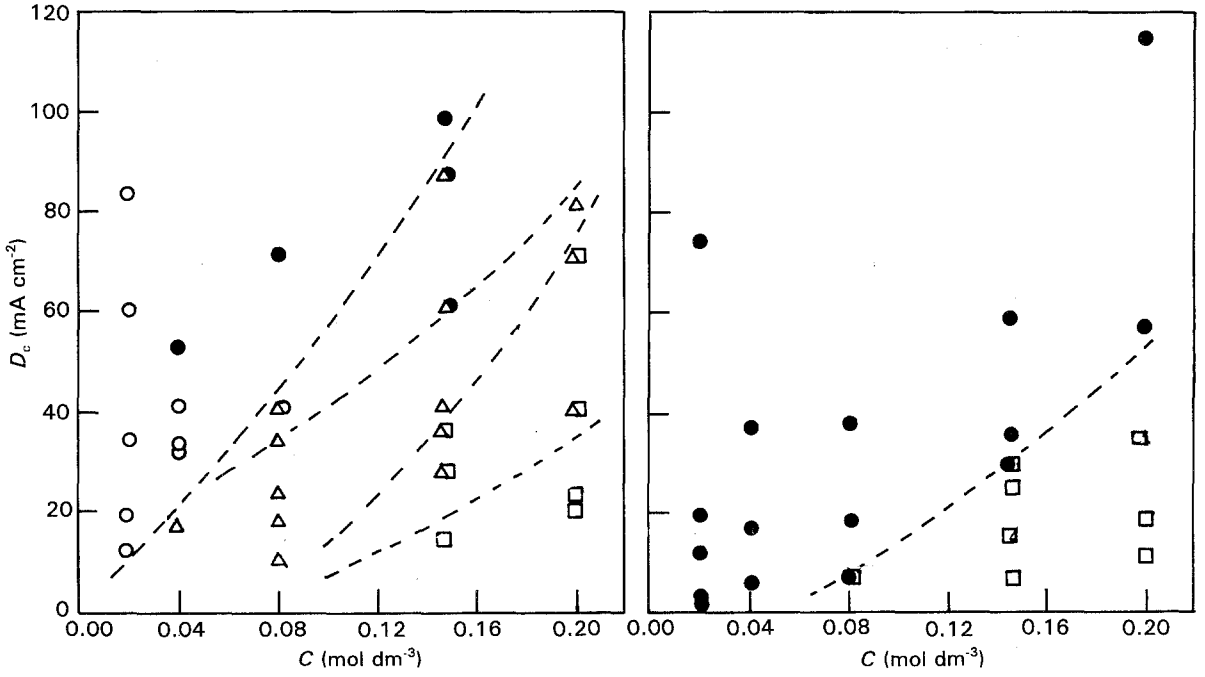

Figure 2 Formation regions of calcium phosphate deposits from $NaNO_3$-added (right) and non-added (left) electrolytes as functions of electrolysis cathode current, D_c, and MCP concentration, C, at 45 °C. (●) Apatite + probably ACP, (○) ACP, (△) $CaHPO_4 \cdot 2H_2O$, (□) $CaHPO_4$.

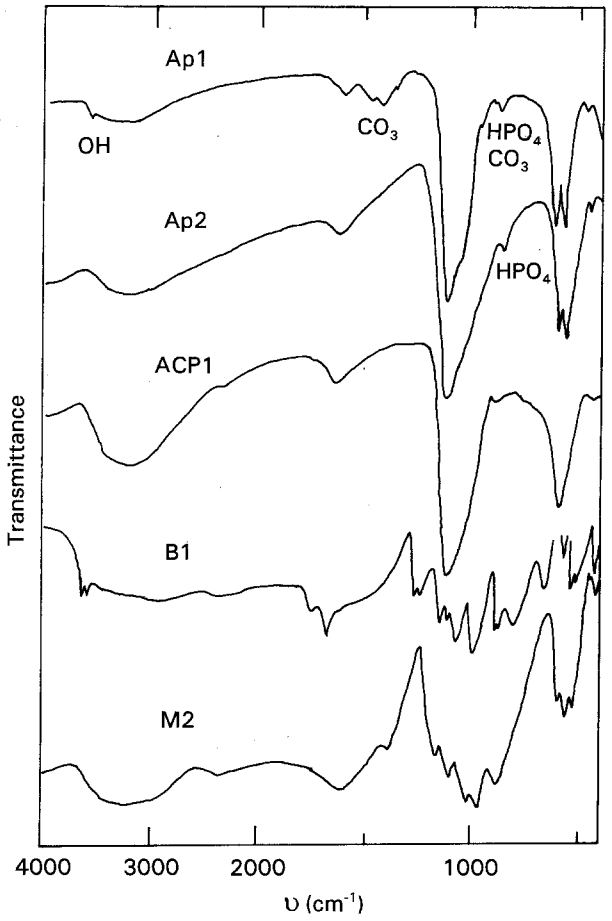

Figure 3 RAS-IR spectra of calcium phosphate deposition layers.

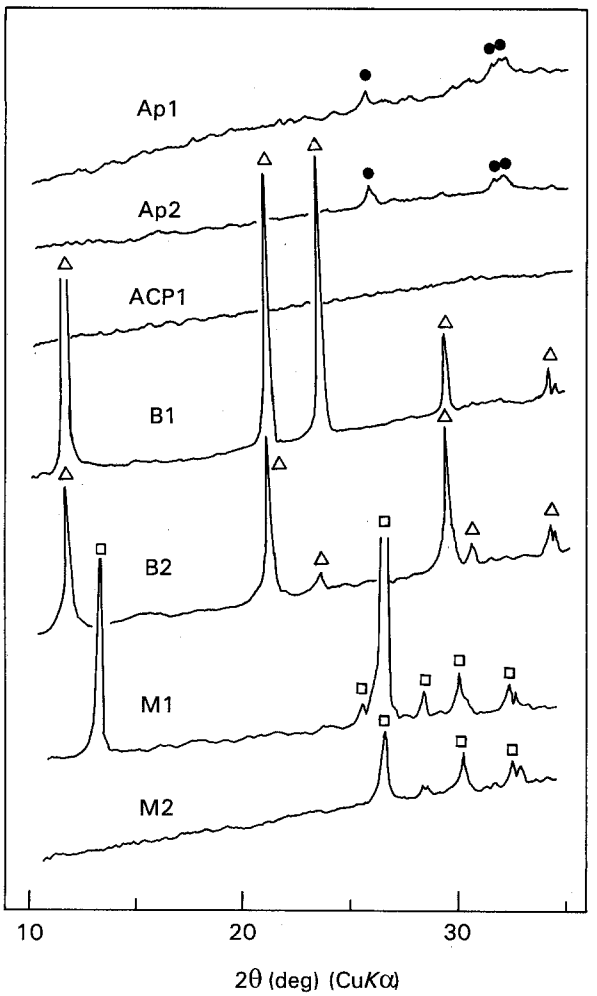

Figure 4 XRD patterns of calcium phosphate deposition layers.

Oriented depositions of $CaHPO_4 \cdot 2H_2O$ and $CaHPO_4$ crystals having a platelet growth tendency were supposed from the patterns for the deposits prepared at low currents. Remarkable changes in the patterns with increasing current suggested that the deposited crystals became fine or unoriented due to the production of a large number of nucleation sites. The crystallinity of the apatite was very low.

3.2. Morphology of the deposits

Figure 5 shows scanning electron micrographs of deposits on the cathode. At relatively low currents, $CaHPO_4 \cdot 2H_2O$ and $CaHPO_4$ plate-like crystals were deposited nearly parallel to the plane of the substrate. At high currents these crystals became fine, as already suggested by the changes in the XRD patterns shown in Fig. 2. The apatite and ACP deposits were very fine grains.

3.3. Composition of apatite

Figure 6 shows EDX spectra for apatite, $CaHPO_4 \cdot 2H_2O$ and $CaHPO_4$ deposits with standard materials. The spectra for $CaHPO_4 \cdot 2H_2O$ and $CaHPO_4$ deposits were observed to be nearly comparable to those for the corresponding standards. The apatite deposit contained sodium. The Ca/P molar ratio of the apatite was estimated to be slightly less than 1.50.

Figures 7 and 8 show XRD patterns and IR spectra of apatite powders scraped from the cathodes. The apatites contained HPO_4^{2-} and CO_3^{2-} groups. Fig. 9 shows TG curves for the powders. The decreases up to 100 °C suggest large amounts of adsorbed H_2O. Decreases up to ~ 600 °C are due to the liberation of adsorbed H_2O and the reactions [7]

$$HPO_4^{2-} \rightarrow 1/2P_2O_7^{4-} + 1/2H_2O\uparrow \quad (1)$$

$$PO_4^{3-} + \text{lattice } H_2O \rightarrow HPO_4^{2-} + OH^- \rightarrow 1/2P_2O_7^{4-} + 1/2H_2O\uparrow + OH^- \quad (2)$$

The formations of $P_2O_7^{4-}$ (IR 730 cm^{-1}) and apatitic OH (IR 3570 cm^{-1}) groups with heating were confirmed by XRD and IR (figures are not shown). The weight decreases at 700–750 °C are characteristic of calcium-deficient hydroxyapatite and known to be due to the reaction

$$P_2O_7^{4-} + 2OH^- \rightarrow 2PO_4^{3-} + H_2O\uparrow \quad (3)$$

accompanying the destruction of apatite to $Ca_3(PO_4)_2$. Products at 900 °C were only $\beta - Ca_3(PO_4)_2$. Therefore, the Ca/P ratios of the apatites were considered to be near 1.50 as well as the value estimated by EDX.

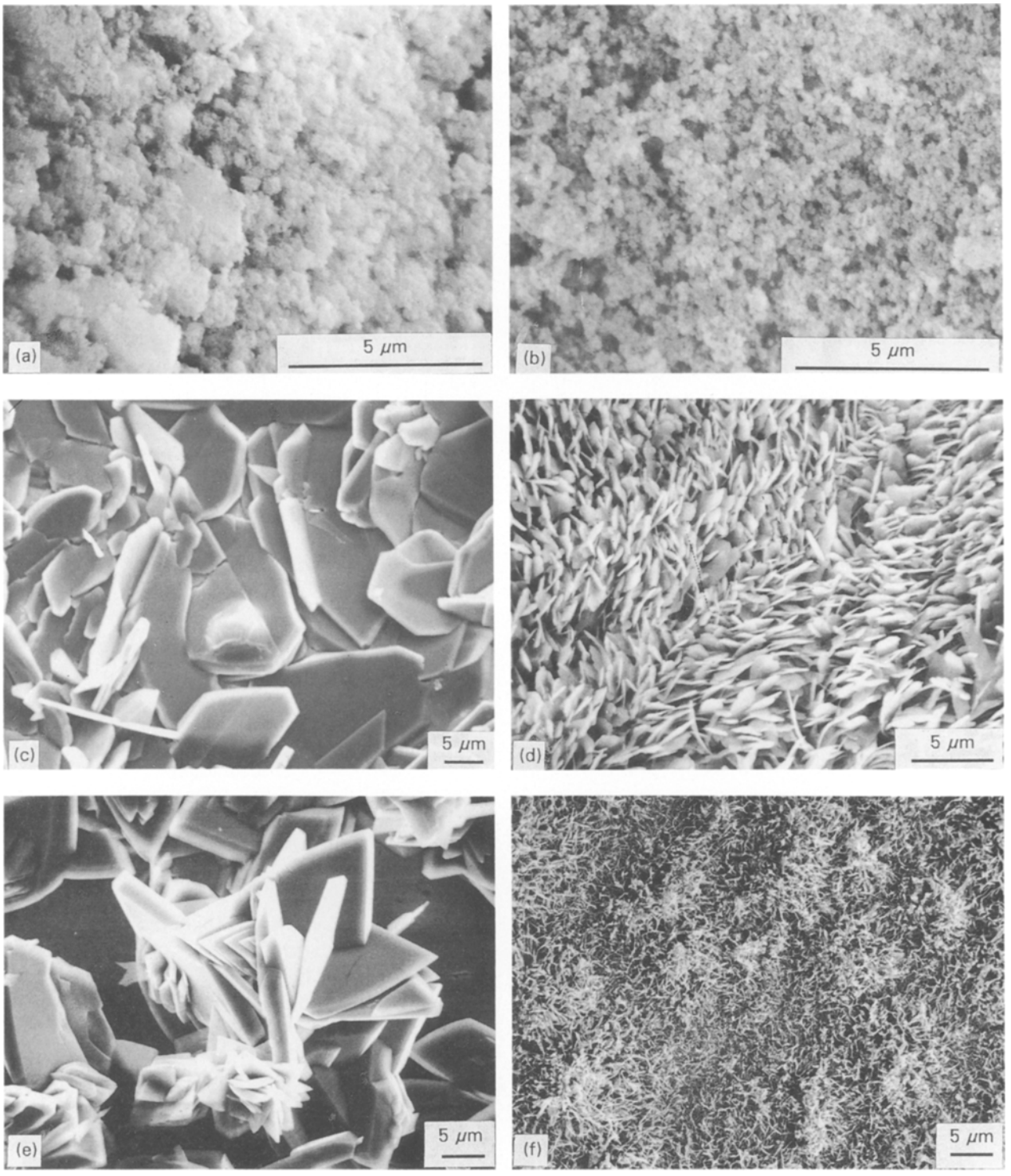

Figure 5 Scanning electron micrographs of calcium phosphate deposits. (a) Ap1, (b) ACP1, (c) B1, (d) B2, (e) M1, (f) M2.

4. Conclusions

Electrolytic calcium phosphate deposits on cathode substrates were prepared by electrolysing acidic $Ca(H_2PO_4)_2 \cdot H_2O$ (MCP) solutions of 0.02–0.21 mol dm^{-3} added with and without $NaNO_3$ at 20–90 °C at cathode currents of 2–200 mA cm^{-2}.

At relatively high MCP concentrations and low currents, $CaHPO_4 \cdot 2H_2O$ and $CaHPO_4$ plate-like crystals below and above ~30 °C, respectively, were deposited nearly parallel to the cathode substrate. With increasing current, the deposits tended to become fine and unoriented. With further increase in current and/or decrease in MCP concentration, apatite deposition became possible. The addition of $NaNO_3$ was effective for enlarging the formation region of apatite. Deposited apatites were very fine grains and had a calcium-deficiency given by a composition such as $(Ca, Na)_9 (HPO_4)(PO_4, CO_3)_5 (OH, H_2O)_2 \cdot nH_2O$ with a Ca/P molar ratio near to 1.50

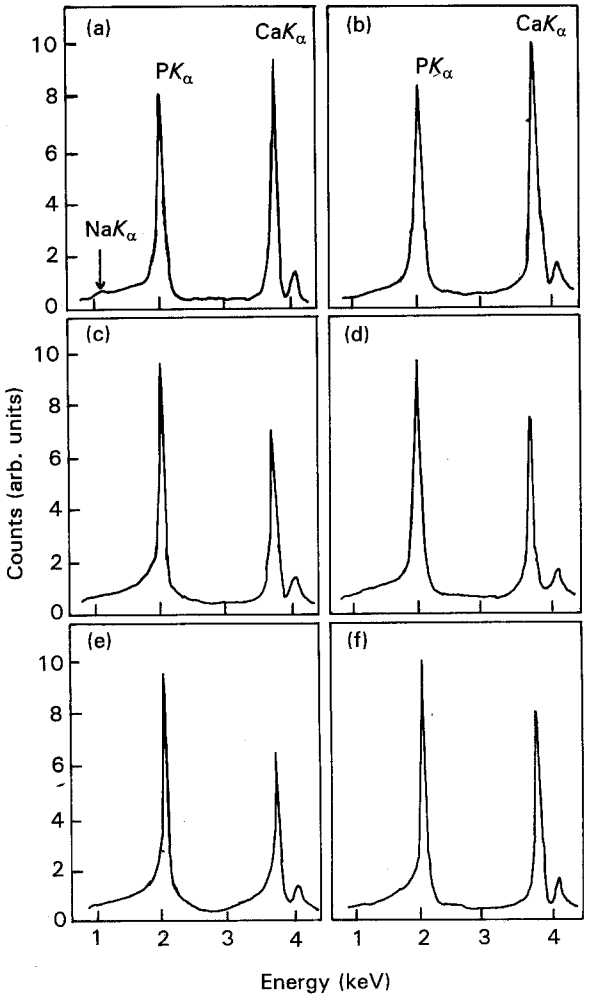

Figure 6 EDX spectra for typical calcium phosphate deposits and standard materials. (a) Ap4, (b) α-$Ca_3(PO_4)_2$, (c) B1, (d) α-$Ca_2P_2O_7$, (e) M2, (f) $CaHPO_4$.

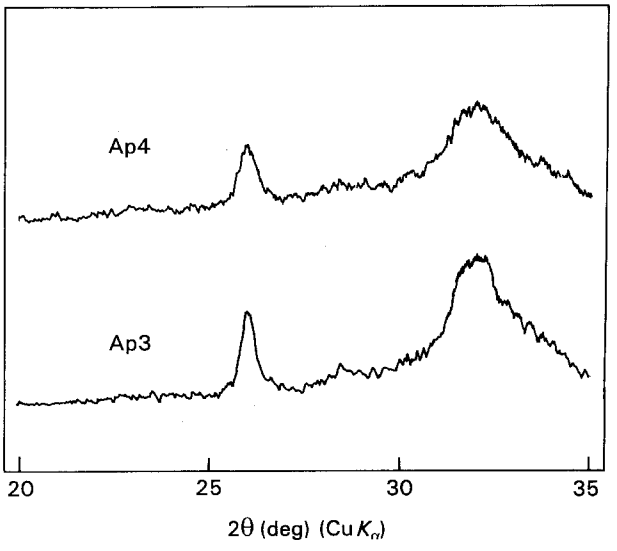

Figure 7 XRD patterns of apatite powders scraped from the cathode.

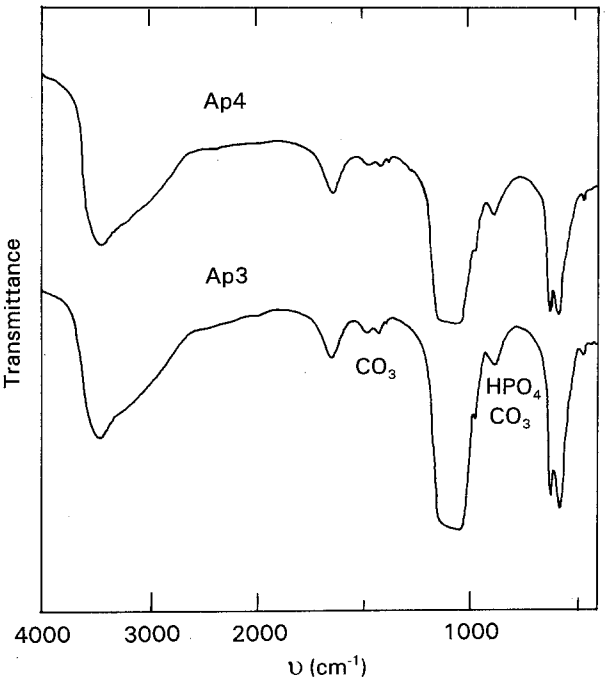

Figure 8 KBr-IR spectra of apatite powders scraped from the cathode.

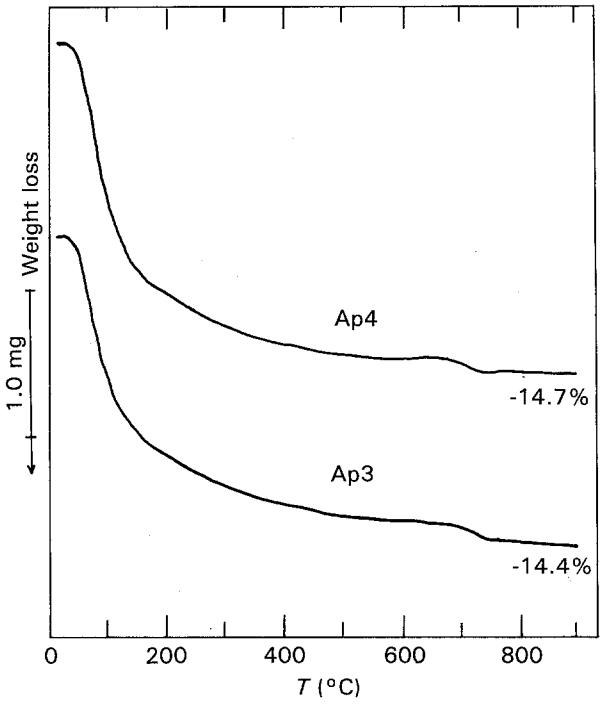

Figure 9 TG curves (10 °C min^{-1}) for apatite powders scraped from the cathode.

References

1. J. REDEPENNING and J. P. McISSAC, *Chem. Mater.* **2** (1990) 625.
2. M. SHIRKHANZADEH, *J. Mater. Sci. Lett.* **10** (1991) 1415.
3. E. D. EANES, *Cacif. Tiss. Res.* **5** (1970) 133.
4. J. D. TERMINE and E. D. EANES, *ibid.* **10** (1972) 171.
5. G. BONEL and G. MONTEL, *C. A. Acad. Sci. Paris* **258** (1964) 923.
6. S. J. JORIS and C. H. AMBERG, *J. Phys. Chem.* **75** (1971) 3172.
7. H. MONMA, S. UENO and T. KANAZAWA, *J. Chem. Tech. Biotechnol.* **31** (1981) 15.

Received 15 December 1992
and accepted 9 September 1993